

Both differential and equatorial heating contributed to African monsoon variations during the mid-Holocene

Ori Adam^{a,*}, Tapio Schneider^b, Yehouda Enzel^a, Jay Quade^c

^a*The Institute of Earth Sciences, The Hebrew University of Jerusalem, Givat Ram, Jerusalem 91904, Israel*

^b*California Institute of Technology, 1200 E. California Blvd., Pasadena, CA 91125, USA*

^c*Department of Geosciences, University of Arizona, 1040 E. 4th Street, Tucson, AZ 85721, USA*

Abstract

The Sahara was significantly greener 11-5 kya and during multiple earlier interglacial periods. But the mechanisms related to the greening of the Sahara remain uncertain as most climate models severely underestimate past wet conditions over north Africa. The variations in the African monsoon related to the greening of the Sahara are thought to be associated with the variations in the inter-hemispheric differential heating of Earth, caused by orbital variations. However, how orbital variations affect regional climate is not well understood. Using recent theory that relates the position of the tropical rain belt to the atmospheric energy budget, we study the effect of orbital forcing during the mid-Holocene on the African monsoon in simulations provided by the third phase of the Paleo Model Intercomparison Project (PMIP3). We find that energy fluxes in the African sector are related to orbital forcing in a complex manner. Contrary to generally accepted theory, orbital modulation of seasonal differential heating alone is shown to be a weak driver of African monsoon variations. Instead, net atmospheric heating near the equator, which modulates the intensity and extent of seasonal migrations of the tropical rain belt, is an important but overlooked driver of African monsoon variations. A conceptual framework that relates African monsoon variations to both equatorial and inter-hemispheric

*Corresponding author

Email address: `ori.adam@mail.huji.ac.il` (Ori Adam)

differential solar heating is presented.

Keywords: PMIP3, African Humid Period, Green Sahara, Atmospheric energy budget, Energy Flux Equator, mid-Holocene

1. Introduction

Extensive geophysical data indicate that the Sahara was significantly wetter and greener during the early and mid-Holocene (11-5 kya) and during multiple earlier interglacial periods [1]. Yet most modern climate models underestimate
5 the past greening of the Sahara, suggesting critical physical processes are misrepresented in these models [2, 3]. The changes in the Saharan precipitation are generally understood to be paced by variations in Earth's orbital parameters, which regulate the differential heating of the hemispheres that drives the seasonal migrations of the tropical rain belt. However, the relation of the zonally
10 uniform changes in insolation caused by orbital variations to regional precipitation variations is not well understood [e.g., 4]. Here, using energetic constraints on the position of the tropical rain belt, we provide a conceptual framework for understanding the relation of orbital variations to different climatic states of the African monsoon.

15 During the wet phase of the Sahara in the early and mid-Holocene, known as the African Humid Period (AHP), parts of the Sahara were vegetated, contained permanent lakes, and sustained human populations in regions that are uninhabitable in the present climate [1, 5]. In part, the AHP is coeval with wet conditions in eastern Africa (the East African Humid Period [6, 7]), which,
20 like the AHP, are not well understood and not well captured by climate models [8, 7, 9]. The drying of the Sahara began around 6 kya. Is generally understood to have occurred alongside cooling in the northern hemisphere (though the extent and timing of the cooling trend remain unclear [10, 11, 8, 12]), as evidenced by various proxies of Sahara and Sahel precipitation [11, 13] and by
25 archaeological findings [14]. The extent and distribution of the greening of the Sahara during the AHP remains a matter of some debate (see [15] for a review).

Nevertheless, most modern climate models underestimate even the low end of plausible greening estimates [16]; they are an order of magnitude short of estimates at the upper end [17, 18]. While the mechanisms behind the discrepancies
30 between models and proxy data remain unclear, improved agreement between simulations and data in some models with vegetation and dust feedbacks suggest surface feedbacks are important for reproducing the greening of the Sahara [19, 20, 21, 22, 23, 24].

Due to the tendency of the tropical rain belt to migrate toward and intensify in a differentially warming hemisphere [25, 26], the greening of the Sahara
35 is generally attributed to Earth’s orbital precession, which modulates seasonal differential heating. However, recent theory, modeling studies, and paleorecords indicate that precession alone cannot explain the greening of the Sahara [3]. First, regional energy fluxes are not clearly related to the zonally-uniform heating associated with orbital variations [27, 28]. Second, modern climate models
40 forced by early- to mid-Holocene insolation (with up to 7% precession-driven increase in boreal summer insolation) tend to underestimate Saharan precipitation relative to proxy reconstructions [16, 3], even when ocean and land feedbacks are included [e.g., 29, 30]. Third, wet Saharan episodes are suggested to have
45 existed during intervals of relatively low boreal summer insolation [e.g., 31, 32].

Here we examine how the regional precipitation and atmospheric energy balance are affected by mid-Holocene orbital changes in models participating in the third phase of the Paleo Model Intercomparison Project (PMIP3 [33]), which is the most extensive modeling study of mid-Holocene conditions to date¹.
50 Our analysis sheds light on the discrepancy between models and reconstructions of the greening of the Sahara and provides a regional perspective on how orbital variations may drive African monsoon climate variations. In particular, our

¹It is important to note, however, that PMIP3 models suffer from severe biases related to misrepresentation of land surface feedbacks, which are critical for capturing monsoonal climate variations. Therefore, while PMIP3 models represent the most extensively coordinated simulation of mid-Holocene conditions to date, they are not free from known biases.

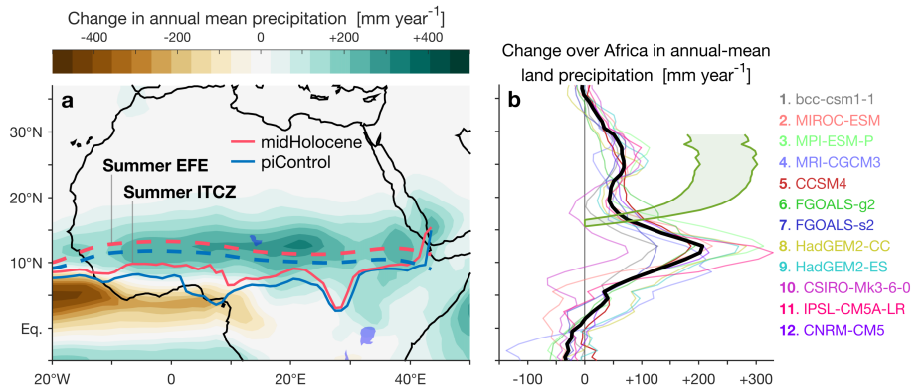


Figure 1: Change in annual-mean precipitation over northern Africa between the mid-Holocene (6 kya) and preindustrial conditions in PMIP3 models. (a) Ensemble-mean change in annual-mean precipitation and the positions of the African ITCZ (solid) and EFE (dashed) in African boreal summer (July–September) during the mid-Holocene (red) and preindustrial conditions (blue). (b) Zonal average of the change in annual-mean precipitation over land (20°W–40°E) for the ensemble mean (thick black) and individual models (colors). Upper and lower estimates of the minimal change in precipitation required to sustain a Saharan steppe during the mid-Holocene are shown shaded in green [34].

results suggest that, in addition to the commonly invoked differential heating of the hemispheres, equatorial heating of the atmosphere is an important factor controlling African monsoon variations.

2. Data and Methods

2.1. Data

Our analysis is based on monthly data from 12 PMIP3 models (Fig. 1) and uses simulations of mid-Holocene and preindustrial conditions. In models for which an ensemble of runs exists, only the first realization of each experiment is analyzed. Seasonal and annual-mean climatologies are calculated from the first available 100 years, interpolated to a $1^\circ \times 1^\circ$ horizontal grid. The boundaries of the African sector are defined as 20°W–40°E. The sector-mean results were found to be qualitatively insensitive to the exact definition of the western

65 and eastern boundaries of the African sector, within a range of $\sim 10^\circ$ of each boundary.

The land cover and dust concentrations in PMIP3 simulations are prescribed to be the same as during preindustrial conditions. This limitation of PMIP3 models may account for the general dry bias in these models over Africa during the mid-Holocene [23]. Specifically, several studies found that vegetation 70 feedbacks and the recycling further north of moisture by increasing the area covered by water bodies amplify the precipitation response to orbital forcing [19, 21, 35, 22], which may then be further amplified by dust feedbacks [23, 24]. However, vegetation feedbacks were included in the earlier generation of PMIP 75 simulation (PMIP2) but were not found to significantly amplify the precipitation response [2]. More generally, these feedbacks were only partially successful in producing the needed latitudinal shift in the rainbelt and in producing the needed change in precipitation intensity.

In this study, rather than assessing the performance of the models, we examine 80 the variation across models in an attempt to provide constraints on the relation between of orbital forcing and African monsoon variations [cf. 36]. This approach has its limitations, since PMIP models both underestimate the range of climate variations [2] and, as mentioned above, misrepresent key physical processes. Nevertheless, we find that the variation across models is sufficient 85 for analyzing the general relation between the African monsoon and the atmospheric energy budget.

2.2. Insolation

The orbital forcing in the PMIP3 simulations is set to mid-Holocene conditions (6 kya). Note, however, that boreal summer (defined here as the months 90 July–September) insolation and the greening of the Sahara peak much earlier, around 9 kya [11]. During the mid-Holocene, peak boreal summer insolation was about 5% greater than today, primarily due to Earth’s precession —at perihelion, the northern hemisphere faced the sun, rather than the southern hemisphere as today. In addition, obliquity was 0.6° higher, and eccentricity

95 was 12% larger. The insolation variations shown below are calculated following the methods described in [37].

2.3. Position Indices

In the zonal mean, the intertropical convergence zone (ITCZ), identified as the latitude of peak tropical precipitation, approximately coincides with the latitude where the zonal-mean northern and southern Hadley cells meet. However, regional manifestations of the ITCZ, for example, in the African sector, are not clearly related to the Hadley circulation (see [38] for a review). Nevertheless, for simplicity, we refer to the latitude of peak African precipitation as a 'regional ITCZ'. Following [39], the latitude of peak zonal- or sector-mean precipitation is estimated as

$$\phi_{\max} = \frac{\int_{30^{\circ}\text{S}}^{30^{\circ}\text{N}} \phi(\cos(\phi)P)^{30}d\phi}{\int_{30^{\circ}\text{S}}^{30^{\circ}\text{N}} (\cos(\phi)P)^{30}d\phi} \quad (1)$$

where ϕ denotes latitude and P denotes precipitation. The 30°S–30°N integration boundaries and power of 30 were found to capture the position of the precipitation maximum well, while reducing grid dependence (see [40] for a sensitivity analysis of Eq. 1).

110 3. The energy flux equator

The ITCZ marks the location of maximal surface mass convergence, and therefore, by mass conservation, the location of the rising branch of the mean meridional overturning circulation [26]. Since energy transport in the deep tropics is dominated by the mean meridional overturning circulation, the ITCZ also approximately marks the latitude of the atmospheric energy flux equator (EFE), where total atmospheric energy transport (AET) vanishes and diverges (i.e., flows away from) [41, 26, 39].

To first order, the position of the EFE (ϕ_{EFE}) is proportional to cross-equatorial AET (AET₀, Fig. 2a) and inversely proportional to a measure of equatorial heating I₀ [42, 26, 27],

$$\phi_{\text{EFE}} = -\frac{1}{a} \frac{\text{AET}_0}{\text{I}_0}. \quad (2)$$

Here a denotes Earth’s radius, the subscript $()_0$ indicates equatorial values, and ϕ_{EFE} , AET_0 , and I_0 can vary in longitude. I is defined as the meridional AET divergence (see the Appendix for details). It is given by the combination of vertical atmospheric net energy input (NEI), energy storage in the atmosphere
125 (ES), and zonal energy input (ZEI),

$$\text{I} \equiv \overbrace{\text{NEI}}^{\text{vertical energy input}} - \overbrace{\text{ES}}^{\text{energy storage}} - \overbrace{\text{ZEI}}^{\text{zonal energy input}}. \quad (3)$$

Here, NEI is given by the sum of net radiative input at the top of the atmosphere, and net radiative, sensible, and latent heat fluxes at the surface; ES is given by the rate of change over time of column-integrated atmospheric sensible and latent heat, and ZEI is given by the zonal gradient of the column-integrated
130 moist static energy flux. See the Appendix and [39, 27] for the derivation of Eqs. (2) and (3) and for more details on the energetic quantities.

The relation of the meridionally varying AET to the EFE, AET_0 and I_0 are depicted in Fig. 2. The sensitivity of the position of the EFE (and hence the ITCZ) to variations in AET_0 and I_0 is depicted in Fig. 3. By assuming that
135 changes in the spatial distribution of tropical precipitation about its peak are small relative to the changes associated with meridional migrations of the rain band, the EFE framework simplifies the analysis of variations in the tropical rain belt to two key parameters: (1) cross-equatorial energy transport (AET_0), which is associated with inter-hemispheric differential heating, and (2) equatorial heating (I_0).
140

The net effect of orbital variations on the atmospheric energy budget is given by the changes in the incoming solar radiation at the top of the atmosphere and by the response of the climate system to these changes. The response is composed of changes in the net radiative balance at the top of the atmosphere, the surface energy budget, energy storage in the atmosphere, and zonal energy
145 fluxes. It is therefore not clear *a priori* how, or if at all, orbital variations affect changes in the zonal-mean or regional differential and equatorial heating, which drive the shifts of the tropical rain belt.

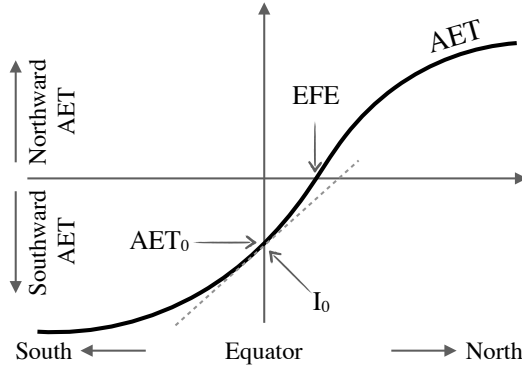


Figure 2: A depiction of atmospheric energy transport (AET) and its relation to the energy flux equator (EFE), cross-equatorial AET and equatorial heating (I_0 , given by the slope of the meridional component of AET at the equator).

Figure 4a shows the zonal-mean changes in insolation and in net atmospheric
 150 energy input (which, in the zonal mean equals the meridional AET divergence I)
 between mid-Holocene and preindustrial conditions in PMIP3 models. The im-
 portance of balancing climatic feedbacks is evident by the lack of a clear relation
 between the orbital forcing (i.e., the change in insolation) and the net response.
 Nevertheless, as expected, net atmospheric energy input in the northern hemi-
 155 sphere increases on average. In addition, equatorial heating is slightly elevated
 on average. As shown in Fig. 4b, the increased differential heating of the north-
 ern hemisphere is balanced by the increase in southward cross-equatorial energy
 flux. This is seen as a negative shift in AET in the tropics, which decreases AET_0
 and shifts the zonal-mean EFE (and with it the ITCZ) northward. However,
 160 both AET_0 and the slope of AET near the equator (i.e., I_0) vary between the
 mid-Holocene and preindustrial conditions. Therefore, from Eq. (2), changes in
 both AET_0 and I_0 (i.e., in both differential and equatorial heating) may have
 played a role in driving shifts in the locations of the African EFE and ITCZ
 during the mid-Holocene.

165 As shown in Fig. 1a, the ensemble-mean shift of the boreal summer ITCZ
 over Africa, induced by mid-Holocene orbital forcing, goes along with a shift in

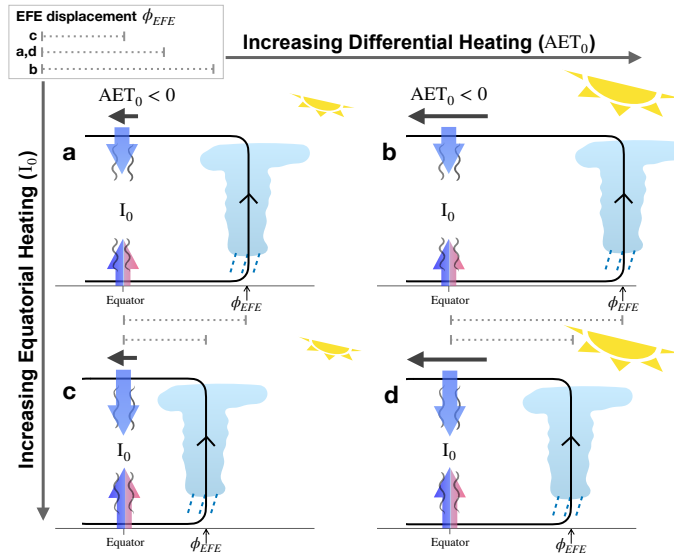


Figure 3: The sensitivity of the position of the EFE (ϕ_{EFE}) to increasing differential heating, resulting in an anomalous cross-equatorial energy fluxes (AET_0), and to increasing equatorial heating (I_0 , the meridional AET divergence at the equator; the red and blue arrows indicate longwave and shortwave radiation), according to Eq. (2). The EFE shifts toward the differentially heated hemisphere. Since differential heating of the northern hemisphere is balanced by southward energy fluxes across the equator, AET_0 is negative in the depicted examples. Increased equatorial heating dampens the migration of the EFE toward the differentially heated hemisphere. Therefore, in the depicted examples, the EFE is nearest to the equator in panel **c** where AET_0 is weakest and I_0 is largest, and is farthest from the equator in panel **b** where AET_0 is strongest and I_0 is weakest. In panels **a** and **d** the EFE is equally displaced because the fractional changes in AET_0 are balanced by the fractional changes in I_0 .

the regional EFE², although the EFE and ITCZ do not exactly coincide. This covariance of the ITCZ and EFE over Africa is also found in observations [27] and simulations [43]. Therefore, variations in the position of the African ITCZ
 170 can be quantitatively linked to variations in the atmospheric energy budget induced by, for example, orbital forcing, ocean variability, or regional feedbacks

²Here the latitude of the EFE is calculated as the latitude of zero crossing of AET. The exact latitude of zero crossing is calculated using a linear interpolation of the two grid points on either side of the zero crossing ([40]).

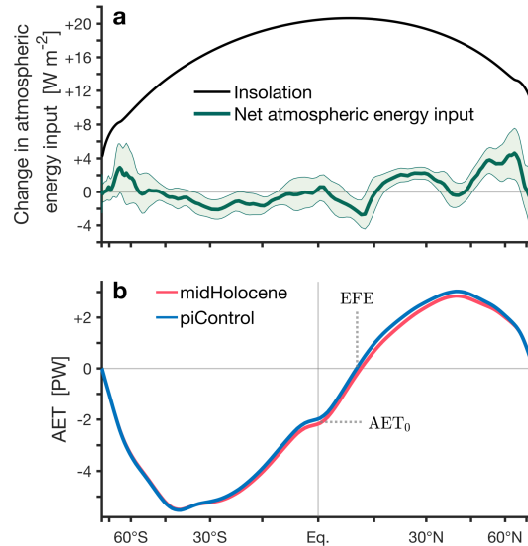


Figure 4: Zonal-mean changes in the PMIP3 ensemble-mean atmospheric energy budget during boreal summer (July–September) for mid-Holocene and preindustrial conditions. (a) Changes in zonal-mean top-of-atmosphere (TOA) incoming solar radiation (black) and net atmospheric energy input (NEI = I in the zonal mean; green, shading indicates ± 1 standard deviation of inter-model spread). (b) Zonal-mean AET during mid-Holocene (red) and preindustrial conditions (blue). The intercept of AET at zero latitude is AET_0 , and its zero is the EFE.

[26, 27]. In what follows, we examine how large regional shifts of the EFE and ITCZ may arise.

4. Regional energetic constraints

175 As expected, a clear northward shift of the annual-mean precipitation over
 Africa is captured in the ensemble mean of PMIP3 models (Fig. 1a; see [44, 45]
 for a detailed analysis). However, all models severely underestimate reconstruc-
 tions of the minimal increase in precipitation required to sustain a Saharan
 steppe: simulated changes do not exceed 100 mm year^{-1} in the mid Sahara, in
 180 disagreement with evidence of widespread grasslands that require an increase
 of at least $200\text{--}300 \text{ mm year}^{-1}$ [Fig. 1b; 34, 16] or lacustrine environments
 [46]. Similarly, the simulated mean position of the African ITCZ during bo-

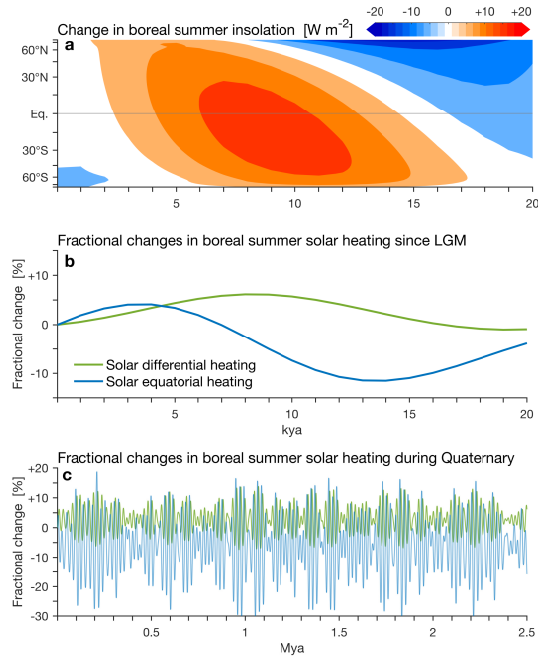


Figure 5: Historic changes in boreal summer insolation. (a) Change from present-day conditions in zonal-mean insolation since the last glacial maximum (LGM). (b,c) Fractional changes (from present day) in differential and equatorial heating since the LGM and during the Quaternary (past 2.5 million years). The insolation variations are calculated following the methods described in [37].

real summer is shifted by about 1 degree, compared with a minimal shift of about 5 degrees required to maintain a Saharan steppe (Fig. 1b; i.e., assuming
 185 the changes in precipitation are caused primarily by changes in the position of the ITCZ, not its intensity or the duration of the wet season). Consistent with reconstructions, most models simulate a wetter eastern Africa (see Fig. S1 for specific models); however, the wetter conditions are not as extensive in equatorial Africa as empirical estimates suggest [6, 7].

190 From Eq. (2), fractional changes in the position of the EFE (and hence the

ITCZ) are given by [26, 42, 47]

$$\frac{\Delta\phi_{\text{EFE}}}{\bar{\phi}_{\text{EFE}}} = \overbrace{\frac{\Delta\text{AET}_0}{\text{AET}_0}}^{\text{shifts caused by differential heating}} - \overbrace{\frac{\Delta\text{I}_0}{\bar{\text{I}}_0}}^{\text{shifts caused by equatorial heating}} \quad (4)$$

where Δ denotes changes between mid-Holocene and preindustrial conditions and the overbar denotes preindustrial conditions. The first term on the rhs of Eq. (4) represents the fractional shift due to changes in cross-equatorial AET induced by inter-hemispheric differential heating. The second term depends on the regional equatorial energy balance (i.e., equatorial heating), which is generally independent of inter-hemispheric differential heating [27, 48, 47] (see section 1 of the SI for a derivation of Eq. 4).

Neglecting the equatorial heating term and assuming regional variations in AET₀ follow the zonal mean, Eq. (4) suggests that the ~5% increase in mid-Holocene boreal summer insolation (and similar decrease in the southern hemisphere, Fig. 5a,b) leads to a ~10% (~1°) shift of the ITCZ position — in accordance with the simulated shifts. More generally, as shown in Fig. 5c, during the Quaternary, changes in differential heating during boreal summer rarely exceed more than 10% relative to preindustrial conditions. This implies that, in contrast to what is widely assumed, in the absence of amplifying feedbacks, orbital differential heating is a weak driver of monsoon climate [e.g., 24, 4]. The lack of regional feedbacks in the African sector likely accounts for the underestimated ITCZ shifts in PMIP3 models, in which identical surface conditions are used in simulations of both the mid-Holocene and preindustrial conditions. However, the typical fractional changes in solar equatorial heating during the Quaternary are of relatively larger magnitude than those in differential heating (Fig. 5c) and may therefore also be important for understanding poleward shifts of the ITCZ. We therefore now turn to examine the potential effects of variations in equatorial heating.

As shown in Fig. 6, the contributions of regional energy storage and zonal energy fluxes to the difference in meridional AET divergence (I) between the mid-Holocene and preindustrial conditions are negligible. Therefore, fractional

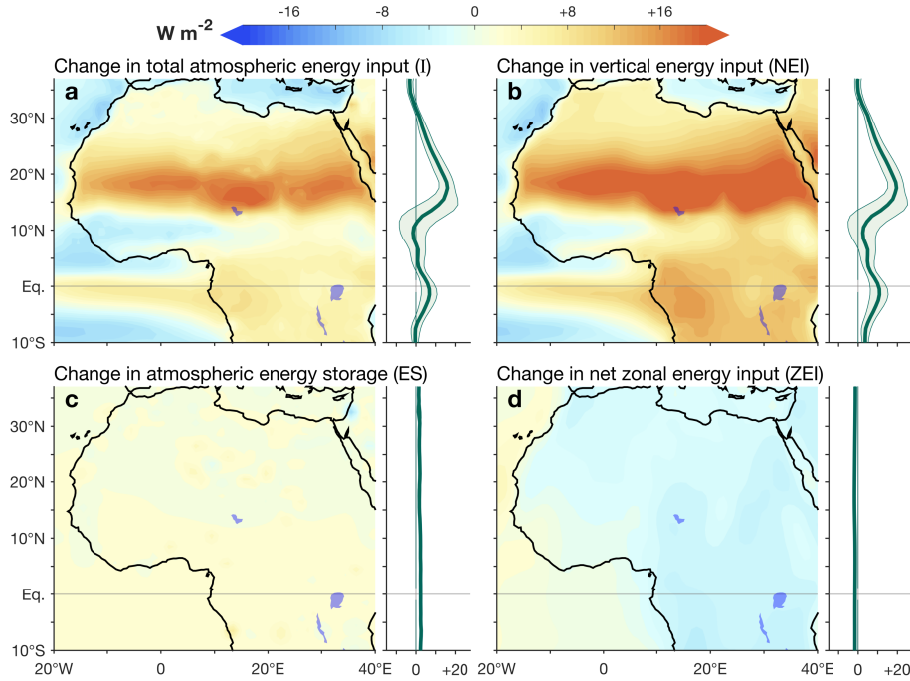


Figure 6: Change in atmospheric energy input during boreal summer (July–September) between mid-Holocene and preindustrial conditions in the African sector. (a) Total atmospheric energy input (I , Eq. 3). (b) Net vertical atmospheric net energy input (NEI), composed of top-of-atmosphere (TOA) net radiative input and surface energy fluxes into the atmosphere. (c) Atmospheric energy storage (ES, the rate of decrease in column-integrated atmospheric sensible and latent heat). (d) Zonal column-integrated energy fluxes (ZEI, the zonal gradient of the atmospheric energy flux). Side panels show zonal means in the African sector (20°W – 40°E), with shaded confidence bounds of 1 standard deviation of intermodel spread.

changes in atmospheric energy input are dominated by the vertical component
 220 (NEI_0) near the equator, i.e.,

$$I_0 \approx \text{NEI}_0. \quad (5)$$

Thus, by neglecting the regional dynamics associated with changes in zonal en-
 ergy transport and energy storage, Eq. (4) simplifies considerably. Specifically,
 fractional variations of NEI_0 can be calculated or estimated from variations in
 the top-of-atmosphere and surface equatorial energy budget, associated with,
 225 for example, orbital forcing, surface radiative and heat fluxes, and cloud feed-

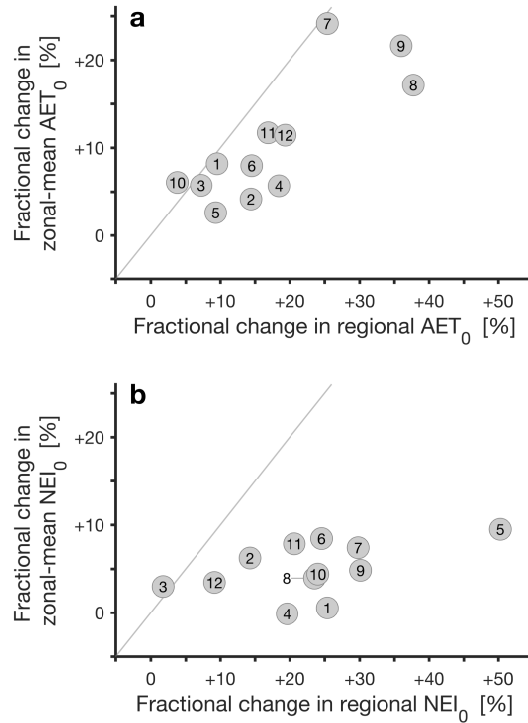


Figure 7: A comparison of zonal-mean vs. African sector-mean (20°W – 40°E) fractional changes between the mid-Holocene and preindustrial control conditions during boreal summer (July–September) in (a) cross-equatorial atmospheric energy transport (AET_0) and (b) equatorial atmospheric net vertical energy input (NEI_0). The identity line is shown in gray. Models are numbered as in Fig. 1.

backs. More generally, variations in NEI_0 dominate the variations in equatorial heating throughout the tropics in PMIP3 models (Fig. S2) and under present-day conditions [48]. This suggests that the approximation (5) can be applied more generally to seasonal and regional variations of the EFE and ITCZ also outside the African sector. Next we examine the relation of differential and equatorial heating to zonal- and sector-mean shifts of the EFE and ITCZ in PMIP3 models.

5. Zonal- and sector-mean variations in PMIP3 models

A comparison of the zonal-mean and African sector-mean fractional changes in AET_0 and NEI_0 is shown in Fig. 7. Even though regional cross-equatorial energy fluxes are not clearly related to the zonally-uniform orbital forcing, the zonal-mean and sector-mean fractional changes in AET_0 are strongly correlated (Fig. 7a, $R = 0.81$). As expected from orbital forcing, the mean fractional change in the zonal-mean AET_0 is 10%, compared with 15% in the African sector. However, these changes vary significantly across models, with maximal and minimal changes of 33% and 2%. Unlike AET_0 , only a weak agreement exists between sector- and zonal-mean fractional changes in NEI_0 ($R=0.49$). The variation across models in sector-mean NEI_0 is also 5 times larger than in the zonal mean. Both zonal- and sector-mean fractional changes in NEI_0 are generally positive. Therefore, from Eq. (4), NEI_0 changes in PMIP3 models damp the poleward shift of the EFE and ITCZ.

The relations of fractional changes in the positions of the African boreal summer EFE and ITCZ and fractional changes in African sector-mean AET_0 and NEI_0 are shown in Fig. 8. Consistent with Eq. (4), fractional changes in the positions of both the EFE and ITCZ are positively correlated with fractional changes in AET_0 ($R=0.77$ and 0.31^* , respectively; the asterisk indicates p -values larger than 0.05.), and negatively but weakly³ correlated with fractional changes in NEI_0 ($R=-0.34^*$ and -0.48^* , respectively). The variance explained by combining the fractional changes of both AET_0 and NEI_0 is 78% for the regional EFE and 36% for the ITCZ. Furthermore, the African EFE and ITCZ positions are well correlated with each other ($R=0.77$). We therefore conclude that both AET_0 and NEI_0 are important predictors of the positions of the EFE and ITCZ in the African sector.

The above results suggest that an empirical model that relates climatic vari-

³Omitting the MPI-ESM-P model (model 3) strengthens the correlation of the ITCZ and EFE with AET_0 and weakens the relation with NEI_0 .

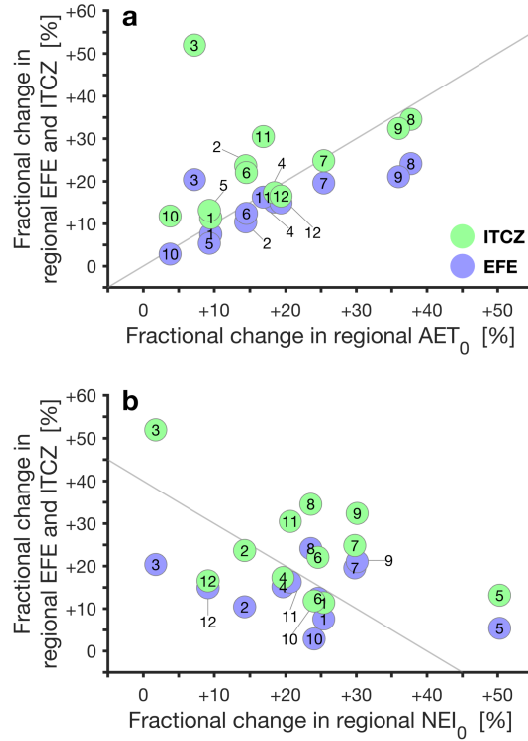


Figure 8: The relation of the fractional changes between the mid-Holocene and preindustrial conditions over Africa (20°W–40°E) in the positions of boreal summer (July–September) EFE (purple) and ITCZ (green), and (a) African sector-mean cross-equatorial atmospheric energy transport AET₀, and (b) equatorial atmospheric net vertical energy input (NEI₀). Models are numbered as in Fig. 1. Reference slope lines of +1 and -1 are shown in gray.

260 ations of the mean position of the ITCZ on seasonal or longer timescales to the
atmospheric energy budget can be written as [47]

$$\delta\phi_{\text{ITCZ}} = \alpha_0\delta\text{AET}_0 + \alpha_1\delta\text{NEI}_0 + \epsilon. \quad (6)$$

Here δ denotes fractional changes and ϵ denotes residual contributions that are uncorrelated with differential and equatorial heating. The empirical constants α_0 and α_1 account for the regional characteristics of the relation of the EFE
265 and ITCZ, which may vary across models, climates, regions, and seasons [49, 50, 26, 39, 27].

Table 1: Summary of the correlation coefficients related to Figs. 7 and 8 and to the regression model Eq. (6). The asterisk indicates p -values above 0.05.

Description	R
Correlation between zonal- and African sector-mean fractional changes in AET_0	0.81
Correlation between zonal- and African sector-mean fractional changes in NEI_0	0.49
Correlation between the EFE and ITCZ over Africa	0.77
Correlation between the EFE and fractional changes in AET_0 over Africa	0.77
Correlation between the ITCZ and fractional changes in AET_0 over Africa	0.31*
Correlation between the EFE and fractional changes in NEI_0 over Africa	-0.34*
Correlation between the ITCZ and fractional changes in NEI_0 over Africa	-0.48*
Correlation between the EFE and the linear regression model (Eq. 6)	0.88
Correlation between the ITCZ and the linear regression model (Eq. 6)	0.62

Using the inter-model spread in fractional changes between the mid-Holocene and preindustrial conditions over Africa, we find $\alpha_0 = 0.4 \pm 0.1$ and $\alpha_1 = -0.5 \pm 0.2$ ($R = 0.62$), where the uncertainty indicates one standard deviation of these coefficients using a leave-one-out cross validation approach. This suggests that PMIP3 models are generally equally sensitive to fractional changes in both NEI_0 and AET_0 ⁴. From Fig. 1, since the mean position of the African ITCZ is $\sim 10^\circ$, for the ITCZ to shift by approximately 5° during the AHP a fractional change of $\sim 50\%$ is required. Given that the expected fractional change in AET_0 associated with orbital forcing is $\sim 10\%$, this shift is likely associated with a decrease in NEI_0 , as opposed to the increased NEI_0 seen in PMIP3 simulations. Quantitatively, in PMIP3 simulations (i.e., for $\alpha_1 = -0.5$) this corresponds to a 70% (or $\sim 15 \text{ Wm}^{-2}$, cf. Fig. S7) mean decrease in NEI_0 . This prediction

⁴The values of α_0 and α_1 are sensitive to the meridional extent of the equatorial averaging of AET_0 and NEI_0 . On average, $\alpha_0 \approx 0.5$ and $\alpha_1 \approx -0.5$ for equatorial averaging of AET_0 and NEI_0 ranging between 5°S – 5°N to 20°S – 20°N . In addition, the value of α_1 is particularly sensitive to the MPI-ESM-P model (data point 3 in Figs. 7 and 8), and reduces to -0.1 in its absence.

is consistent with the paleo precipitation model of [47], which, as in Eq. (6),
280 relates the position of the ITCZ to orbital variations, but also includes the
effect of tropical heating on moisture availability [51]. Using this model, a
50% reduction in NEI_0 produced an annual-mean difference between the mid-
Holocene and preindustrial conditions similar to that found by [34] (Fig. 1b).
Additionally, unlike AET_0 , relatively large fractional changes in NEI_0 do not
285 require large absolute variations. Since NEI_0 is the net of large balancing terms,
large fractional changes of NEI_0 (i.e., above 50%) require only relatively small
changes in, e.g., cloud effects or surface latent heat fluxes (cf. section 2 of the
SI).

6. Discussion and Conclusions

290 African monsoon variations are commonly conceptualized as meridional shifts
of the continental ITCZ in the African sector. Based on the tendency of the
ITCZ to migrate toward the differentially warming hemisphere, these shifts and
similar shifts in the tropical rain belt outside the African sector are traditionally
associated with changes in the inter-hemispheric differential heating of Earth.
295 We have shown that changes in the equatorial heating of the atmosphere, which
modulates both precipitation intensity by affecting moisture availability [51, 47]
and the extent of ITCZ migrations (Eq. 4), contributes to ITCZ variations
comparable to those induced by differential heating alone. Incorporating this
important and often overlooked driver of African monsoon variations therefore
300 seems important for understanding wet Saharan episodes.

The relation of the regional ITCZ position and the atmospheric energy bud-
get can be understood in the framework of the covariance of the ITCZ with
the regional energy flux equator (EFE, Fig. 1). To first order, variations
of the regional ITCZ on timescales of a season or longer are proportional to
305 cross-equatorial atmospheric energy transport (AET_0) associated with inter-
hemispheric differential heating, and inversely proportional to equatorial heat-
ing [2; for a review see 26]. However, as shown in Figs. 4 and 7, due to climatic

feedbacks, the effect of orbital forcing on zonal-mean or regional energy fluxes cannot be accurately inferred from the associated variations in incoming solar
310 radiation.

In PMIP3 models, differential heating and the associated cross-equatorial AET only partly account for the meridional shifts of the ITCZ. Equatorial heating, which modulates the extent of seasonal ITCZ migrations [Eq. 4; 42, 26, 39, 47], is found to be an additional important driver of ITCZ shifts. Given the
315 sensitivity of the regional position of the ITCZ to regional feedbacks, which may also vary in their representation across climate models, an empirical regression model which includes the effects of both differential and equatorial heating is presented in Eq. (6). The contribution of equatorial heating variations (δNEI_0) to variations in the position of the ITCZ has been ignored in most previous
320 empirical studies of the ITCZ position, where the relation of the ITCZ position to the atmospheric energy budget is assumed to be solely dependent on AET_0 [i.e., assuming $\alpha_1 = 0$ in Eq. 6; e.g., 52, 53, 50, 54]. By including processes which are not related to differential heating, Eq. (6) provides a simple yet critical generalization of empirical models of ITCZ migrations. A summary of
325 the correlation coefficients pertaining to the relation of the EFE and ITCZ to differential (AET_0) and equatorial heating (NEI_0) in PMIP3 models (Figs. 7 and 8) and to the regression model (Eq. 6) is presented in Table 1.

An appreciable amount of the variance in the position of the African boreal-summer ITCZ is not accounted for by the extended regression model (Fig. 8),
330 implying that processes other than meridional shifts of the ITCZ cannot be neglected. Indeed, extensive literature exists on regional mechanisms associated with the AHP [for a review see 3]. Prime examples include the ‘monsoon-desert mechanism’, which links the invigoration of the Indian monsoon with enhanced descent and hence suppressed precipitation over northern Africa [55];
335 the ‘ventilation mechanism’, in which increases in precipitation are limited by the decreased relative humidity of the warming African continent relative to the Atlantic [56]; the dynamics of moisture fluxes from the Atlantic and the Mediterranean [e.g., 57, 58]; dynamical effects of the African heat low [e.g.,

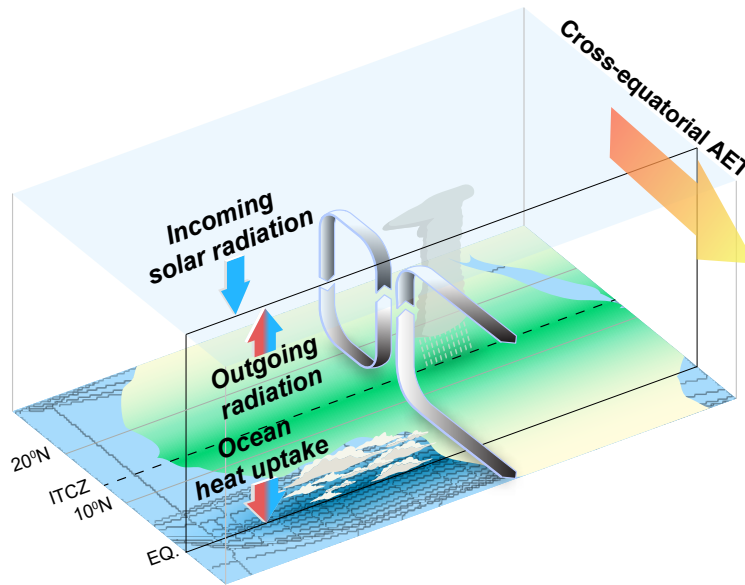


Figure 9: Energy fluxes controlling ITCZ shifts in the African sector. Variations in cross-equatorial atmospheric energy transport (AET), associated with inter-hemispheric differential heating, force the ITCZ to migrate towards the differentially heated hemisphere. Atmospheric equatorial heating modulates precipitation intensity and the extent of the ITCZ migrations. The net equatorial heating is determined primarily by the radiative balance at the top of the atmosphere and ocean heat uptake, composed of longwave and shortwave radiative fluxes (red and blue arrows, respectively) as well as sensible and latent heat fluxes near the surface.

59, 60, 61]; and vegetation and dust feedbacks [e.g., 29, 24].

340 Nevertheless, the extended theory (Eq. 6) captures over 30% of the variance of the ITCZ in PMIP3 models, compared with about 20% when only differential heating is considered. Moreover, since equatorial heating modulates the extent of seasonal ITCZ migrations (Eq. 2, Fig. 3), variations in equatorial heating provide a conceptual framework for understanding hemispherically symmetric
 345 variations in precipitation [62], such as those observed over Africa since the last glacial maximum [63] and in the Pacific during the Little Ice Age [64]. Furthermore, the unique shape of the African continent makes the African monsoon (in particular the West African monsoon) sensitive to variations in the equatorial eastern Atlantic. The net equatorial heating over the eastern Atlantic is

350 regulated by cloud feedbacks, which are not well understood, but which a grow-
ing body of evidence suggests may be positive (i.e., low-cloud cover increases
as the surface cools, [65, 66]). Tropical low-cloud radiative cooling exceeding
10 W m⁻² (i.e., the amount required to shift the African ITCZ by several
degrees) is well within the potential radiative response by clouds to the equa-
355 torial surface cooling during the AHP that is suggested by reconstructions and
models [Fig. S5; 66, 67] (though estimates of the temperature trends in the
equatorial eastern Atlantic remain inconclusive [68, 69, 67]). However, modern
climate models significantly underestimate low-cloud cover and overestimate
the equatorial heating in the eastern Atlantic during boreal summer [48]. In
360 the models, this reduces the fractional changes in equatorial heating during the
mid-Holocene, thus dampening the response of the African monsoon to orbital
variations (Eq. 4, Figs. 7 and 8).

Similarly, vegetation and dust feedbacks (which are not present in PMIP3
models), alter the surface radiative and latent heat fluxes [21, 24] and may am-
365 plify regional cross-equatorial AET and hence ITCZ shifts. The regional surface
fluxes may also enhance the differential heating of the African continent relative
to the Atlantic (cf. the land-sea contrast in Fig. 6) during periods of enhanced
boreal insolation, thus amplifying the contribution of zonal moisture fluxes from
the Atlantic [70, 71, 72, 73] — an aspect not covered by the framework presented
370 here.

The factors controlling ITCZ shifts in the African sector are depicted in
Fig. 9. The ITCZ shifts towards the differentially heated hemisphere, inducing
regional cross-equatorial AET (AET₀), which balances the differential heating.
The precipitation intensity and the extent of the ITCZ migrations are modu-
375 lated by equatorial heating (NEI₀). The equatorial heating is dominated by
net radiative input at the top of the atmosphere (TOA, Fig. S3) and surface
energy fluxes into the atmosphere (Figs. S4-5), which are both strongly coupled
to cloud feedbacks⁵.

⁵In addition, due to the low continental heat capacity, changes in surface energy fluxes

The regional framework presented here challenges the general conception
 380 that orbital modulation of inter-hemispheric differential heating is the primary
 driver of AHPs; instead, it points to the important role of equatorial heating
 and offers a more nuanced picture that incorporates the regional characteristics
 of the African sector. Since vertical atmospheric energy input dominates the
 atmospheric energy budget also outside the African sector (Figs. S3-5), the
 385 regional approach presented here may be generalizable to other sectors.

Acknowledgments

The PMIP3 data was downloaded from Earth System Grid Federation (ESGF).
 Ori Adam acknowledges support by the Israeli Science Foundation grant 1185/17.

Appendix

390 The variations in the heating of the atmosphere (NEI), which ultimately
 drive the shifts of the African monsoon, are related to atmospheric energy trans-
 port (AET) by the energy balance equation of the atmosphere (e.g., [27])

$$\text{div}(\text{AET}) = \text{NEI} - \text{ES} \quad (7)$$

where $\text{div}(\cdot)$ denotes the divergence. Atmospheric energy storage (ES) is gener-
 ally negligible on annual or longer timescales [50], but it can be significant on
 395 seasonal timescales and is therefore included in our analysis.

In order to allow for regional variations, zonal energy input into the African
 sector must also be considered. As mentioned in the Discussion, the zonal over-
 turning circulation in the African sector also contributes to the mean precipi-
 tation. However, given the zonal orientation of the ITCZ in the African sector
 400 (e.g., Fig. 1), it is reasonable to assume predominantly Hadley-like circulation
 (Fig. 9) in the African sector. The energy balance equation can be written as
 [27],

$$\partial_y \text{AET} = \text{NEI} - \text{ES} - \partial_x \text{AET} \quad (8)$$

over land are negligible relative to changes in ocean heat uptake [26]

where $-\partial_x \text{AET}$ denotes column-integrated zonal energy input across atmospheric columns (this term vanishes in the zonal mean). (Cartesian notation
 405 is used here only for simplicity; the calculations presented in the results are done in spherical coordinates.) The rhs of Eq. (8) therefore describes the local net energy input into the atmosphere, defined here as $I \equiv \partial_y \text{AET}$.

Using Eq. (8), a first-order Taylor expansion of AET about the equator gives [42]

$$\text{AET} \approx \text{AET}_0 + I_0 \cdot (a\phi) \quad (9)$$

410 where $()_0$ denotes equatorial average. It is therefore readily shown that the latitude where AET vanishes (i.e., the latitude of the energy flux equator EFE) is given by Eq. (2).

From Eq. (8), the difference in the net heating between the hemispheres is equal to the zonal-mean cross-equatorial AET. In addition, since ITCZs are
 415 located in regions of strong surface convergence and upper-level divergence, it is useful to consider only the divergent component of the energy flux. Therefore, regional cross-equatorial AET, denoted here as AET_0 , is calculated as the average between 5°S – 5°N of the divergent component of AET, derived from Eq. (7) [27]. In the zonal mean, AET_0 can be directly calculated from the imbalance
 420 in I between the hemispheres. Similarly, local equatorial heating, denoted here as I_0 , is calculated as the equatorial average (10°S – 10°N) of I . The results were found to be qualitatively insensitive to the meridional extent of the equatorial average if it does not exceed 20° . See [27] for specific details on the calculation of the energetic quantities.

425 **References**

- [1] P. deMenocal, J. Ortiz, T. Guilderson, J. Adkins, M. Sarnthein, L. Baker, M. Yarusinsky, Abrupt onset and termination of the African Humid Period: rapid climate responses to gradual insolation forcing, *Quaternary Sci. Rev.* 19 (2000) 347–361.

- 430 [2] S. P. Harrison, P. J. Bartlein, S. Brewer, I. C. Prentice, M. Boyd, I. Hessler, K. Holmgren, K. Izumi, K. Willis, Climate model benchmarking with glacial and mid-holocene climates, *Climate Dynamics* 43 (3) (2014) 671–688. doi:10.1007/s00382-013-1922-6.
URL <https://doi.org/10.1007/s00382-013-1922-6>
- 435 [3] M. Claussen, A. Dallmeyer, J. Bader, Theory and modeling of the African humid period and the green Sahara, *Oxford Research Encyclopedia of Climate Science* doi:10.1093/acrefore/9780190228620.013.532.
- [4] X. Liu, D. S. Battisti, A. Donohoe, Tropical precipitation and cross-equatorial ocean heat transport during the mid-Holocene, *Journal of Climate* 30 (10) (2017) 3529–3547. doi:10.1175/JCLI-D-16-0502.1.
440
- [5] R. Kuper, S. Kröpelin, Climate-controlled Holocene occupation in the Sahara: Motor of Africa’s evolution, *Science* 313 (5788) (2006) 803–807. arXiv:<http://science.sciencemag.org/content/313/5788/803.full.pdf>, doi:10.1126/science.1130989.
445 URL <http://science.sciencemag.org/content/313/5788/803>
- [6] F. Gasse, Hydrological changes in the African tropics since the Last Glacial Maximum, *Quaternary Sci. Rev.* 19 (2000) 189–211.
- [7] J. E. Tierney, S. C. Lewis, B. I. Cook, A. N. LeGrande, G. A. Schmidt, Model, proxy and isotopic perspectives on the east african humid period, *Earth and Planetary Science Letters* 307 (1) (2011) 103 – 112.
450 doi:<https://doi.org/10.1016/j.epsl.2011.04.038>.
URL <http://www.sciencedirect.com/science/article/pii/S0012821X11002652>
- [8] Z. Liu, J. Zhu, Y. Rosenthal, X. Zhang, B. L. Otto-Bliesner, A. Timmermann, R. S. Smith, G. Lohmann, W. Zheng, O. E. Timm, The Holocene temperature conundrum, *Proc. Natl. Acad. Sci.* 111 (2014) E3501–E3505.
455 doi:0.1073/pnas.1407229111.

- [9] Z. Liu, S. P. Harrison, J. Kutzbach, B. Otto-Bliesner, Global monsoons in the mid-holocene and oceanic feedback, *Climate Dynamics* 22 (2) (2004) 157–182. doi:10.1007/s00382-003-0372-y.
460 URL <https://doi.org/10.1007/s00382-003-0372-y>
- [10] H. Renssen, H. Sepp, X. Crosta, H. Goosse, D. Roche, Global characterization of the holocene thermal maximum, *Quaternary Science Reviews* 48 (Supplement C) (2012) 7 – 19. doi:<https://doi.org/10.1016/j.quascirev.2012.05.022>.
465 URL <http://www.sciencedirect.com/science/article/pii/S0277379112002168>
- [11] S. A. Marcott, J. D. Shakun, P. U. Clark, A. C. Mix, A reconstruction of regional and global temperature for the past 11,300 years, *Science* 339 (2013) 1198–1201.
470
- [12] J. Marsicek, B. N. Shuman, P. J. Bartlein, S. L. Shafer, S. Brewer, Reconciling divergent trends and millennial variations in holocene temperatures, *Nature* 554 (2018) 92–96. doi:10.1038/nature25464.
- [13] T. M. Shanahan, N. P. McKay, K. A. Hughen, J. T. Overpeck, B. Otto-Bliesner, C. W. Heil, J. King, C. A. Scholz, J. Peck, The time-transgressive termination of the African Humid Period, *Nature Geosci.*doi:10.1038/NGEO2329.
475
- [14] K. Manning, A. Timpson, The demographic response to holocene climate change in the sahara, *Quaternary Science Reviews* 101 (Supplement C) (2014) 28 – 35. doi:<https://doi.org/10.1016/j.quascirev.2014.07.003>.
480 URL <http://www.sciencedirect.com/science/article/pii/S0277379114002728>
- [15] J. Quade, E. Dente, M. Armon, Y. B. Dor, E. Morin, O. Adam, Y. Enzel, Megalakes in the sahara? a review., *Quaternary Research* 90 (2) (2018) 253–275. doi:10.1017/qua.2018.46.
485

- [16] S. Joussaume, K. E. Taylor, P. Braconnot, J. F. B. Mitchell, J. E. Kutzbach, S. P. Harrison, I. C. Prentice, A. J. Broccoli, A. Abe-Ouchi, P. J. Bartlein, C. Bonfils, B. Dong, J. Guiot, K. Herterich, C. D. Hewitt, D. Jolly, J. W. Kim, A. Kislov, A. Kitoh, M. F. Loutre, V. Masson, B. McAvaney, N. McFarlane, N. de Noblet, W. R. Peltier, J. Y. Peterschmitt, D. Pollard, D. Rind, J. F. Royer, M. E. Schlesinger, J. Syktus, S. Thompson, P. Valdes, G. Vettoretti, R. S. Webb, U. Wyputta, Monsoon changes for 6000 years ago: Results of 18 simulations from the Paleoclimate Modeling Intercomparison Project (PMIP), *Geophys. Res. Lett.* 26 (1999) 859–862.
- [17] S. J. Armitage, N. A. Drake, S. Stokes, A. El-Hawat, M. J. Salem, K. White, P. Tunner, S. J. McLaren, Multiple phases of north african humidity recorded in lacustrine sediment from the fezzan basin, libyan sahara, *Quaternary Geochronology* 2 (2007) 181–186.
- [18] N. Drake, R. M. Blench, S. J. Armitage, C. S. Bristow, K. H. White, Ancient watercourses and biogeography of the sahara explain the peopling of the desert, *Proceedings of the National Academy of Sciences* 108 (2011) 458–462.
- [19] M. Claussen, V. Gayler, The greening of the sahara during the mid-Holocene: Results of an interactive atmosphere-biome model, *Global Ecol. Biogeogr. Lett.* 6 (1997) 369–377. doi:10.2307/2997337.
- [20] S. Levis, G. B. Bonan, C. Bonfils, Soil feedback drives the mid-Holocene north African monsoon northward in fully coupled ccsm2 simulations with a dynamic vegetation model, *Climate Dynamics* 23 (2014) 791802. doi:10.1007/s00382-004-0477-y.
- [21] C. M. Patricola, K. H. Cook, Dynamics of the west african monsoon under mid-Holocene precessional forcing: Regional climate model simulations, *J. Climate* 20 (2007) 694–716. doi:10.1175/JCLI4013.1.
- [22] A. L. S. Swann, I. Y. Fung, Y. Liu, J. C. H. Chiang, Remote vegetation

- 515 feedbacks and the mid-Holocene green Sahara, *J. Climate* 27 (2014) 4857–
4870. doi:10.1175/JCLI-D-13-00690.1.
- [23] F. S. Pausata, G. Messori, Q. Zhang, Impacts of dust reduction on the
northward expansion of the african monsoon during the green sahara
period, *Earth and Planetary Science Letters* 434 (2016) 298 – 307.
520 doi:<https://doi.org/10.1016/j.epsl.2015.11.049>.
URL [http://www.sciencedirect.com/science/article/pii/
S0012821X15007530](http://www.sciencedirect.com/science/article/pii/S0012821X15007530)
- [24] M. Gaetani, G. Messori, Q. Zhang, C. Flamant, F. S. R. Pausata, Un-
derstanding the mechanisms behind the northward extension of the West
525 African monsoon during the mid Holocene, *Journal of Climate* 30 (19)
(2017) 7621–7642. doi:10.1175/JCLI-D-16-0299.1.
- [25] J. C. H. Chiang, A. R. Friedman, Extratropical cooling, interhemispheric
thermal gradients, and tropical climate change, *Ann. Rev. Earth Planet.
Sci.* 40 (2012) 383–412.
- 530 [26] T. Schneider, T. Bischoff, G. H. Haug, Migrations and dynamics of the
intertropical convergence zone, *Nature* 513 (2014) 45–53. doi:10.1038/
nature13636.
- [27] O. Adam, T. Bischoff, T. Schneider, Seasonal and interannual variations
of the energy flux equator and ITCZ. Part II: Zonally varying shifts of the
535 ITCZ, *J. Climate* 29 (2016) 7281–7293. doi:10.1175/JCLI-D-15-0710.1.
- [28] W. H. G. Roberts, P. J. Valdes, J. S. Singarayer, Can energy fluxes be
used to interpret glacial/interglacial precipitation changes in the tropics?,
Geophys. Res. Lett. 44 (2017) 6373–6382. doi:10.1002/2017GL073103.
- [29] TEMPO, Potential role of vegetation feedback in the climate sensitivity of
540 high-latitude regions: A case study at 6000 years b.p., *Global Biogeochem-
ical Cycles* 10 (4) (1996) 727–736. doi:10.1029/96GB02690.

- [30] J. E. Kutzbach, Z. Liu, Response of the African monsoon to orbital forcing and ocean feedbacks in the middle Holocene, *Science* 278 (1997) 440–443.
- [31] A.-M. Lézine, J. Casanova, Correlated oceanic and continental records demonstrate past climate and hydrology of north africa (0-140 ka), *Geology* 19 (4) (1991) 307–310.
- [32] I. S. Castañeda, S. Mulitza, E. Schefu, R. A. Lopes dos Santos, J. S. Sinninghe Damsté, S. Schouten, Wet phases in the Sahara/Sahel region and human migration patterns in North Africa, *Proceedings of the National Academy of Sciences* 106 (48) (2009) 20159–20163. arXiv:<http://www.pnas.org/content/106/48/20159.full.pdf>, doi:10.1073/pnas.0905771106.
URL <http://www.pnas.org/content/106/48/20159.abstract>
- [33] P. Braconnot, S. P. Harrison, B. Otto-Bliesner, A. Abe-Ouchi, J. Jungclauss, J. Y. Peterschmitt, Vol. Vol. 16, International CLIVAR Project Office, Southampton, United Kingdom.
- [34] D. Jolly, S. P. Harrison, B. Damnati, R. Bonnefille, Simulated climate and biomes of Africa during the late Quaternary: Comparison with pollen and lake status data, *Quat. Sci. Rev.* 17 (1998) 629–6657.
- [35] G. Krinner, A.-M. Lzine, P. Braconnot, P. Sepulchre, G. Ramstein, C. Grenier, I. Gouttevin, A reassessment of lake and wetland feedbacks on the north african holocene climate, *Geophysical Research Letters* 39 (7). doi:10.1029/2012GL050992.
- [36] M. R. Allen, W. J. Ingram, Constraints on future changes in climate and the hydrologic cycle, *Nature* 419 (2002) 224–232.
- [37] P. Huybers, I. Eisenman, Integrated summer insolation calculations, NOAA/NCDC paleoclimatology program, Available online at ftp://ftp.ncdc.noaa.gov/pub/data/paleo/climate_forcing/

orbital_variations/huybers2006insolation/huybers2006b.txt

570

(2006).

- [38] S. E. Nicholson, The ITCZ and the seasonal cycle over equatorial africa, *Bulletin of the American Meteorological Society* 99 (2) (2018) 337–348. doi:10.1175/BAMS-D-16-0287.1.
- [39] O. Adam, T. Bischoff, T. Schneider, Seasonal and interannual variations of
575 the energy flux equator and ITCZ. Part I: Zonally averaged ITCZ position,
J. Climate 29 (2016) 3219–3230. doi:10.1175/JCLI-D-15-0512.1.
- [40] O. Adam, K. M. Grise, P. Staten, I. R. Simpson, S. M. Davis, N. A. Davis,
D. W. Waugh, T. T. Birner, A. Ming, The TropD software package (v1):
standardized methods for calculating tropical-width diagnostics, *Geosci.*
580 *Model Dev.* 11 (2018) 4339–4357. doi:10.5194/gmd-11-4339-2018.
- [41] S. M. Kang, D. M. W. Frierson, I. M. Held, The tropical response to extra-
tropical thermal forcing in an idealized GCM: The importance of radiative
feedbacks and convective parameterization, *J. Atmos. Sci.* 66 (2009) 2812–
2827.
- 585 [42] T. Bischoff, T. Schneider, Energetic constraints on the position of the
Intertropical Convergence Zone, *J. Climate* 27 (2014) 4937–4951. doi:
10.1175/JCLI-D-13-00650.1.
- [43] R. Shekhar, W. R. Boos, Improving energy-based estimates of monsoon
location in the presence of proximal deserts, *J. Climate* 29 (2016) 4741–
590 4761. doi:10.1175/JCLI-D-15-0747.1.
- [44] S. Harrison, P. Bartlein, K. Izumi, G. Li, J. Annan, J. Hargreaves,
P. Braconnot, M. Kageyama, Evaluation of cmip5 palaeo-simulations to
improve climate projections, *Nat. Clim. Chang.* 5 (2015) 735743. doi:
10.1038/nclimate2649.
- 595 [45] M. Chevalier, S. Brewer, B. M. Chase, Qualitative assessment of pmip3
rainfall simulations across the eastern african monsoon domains during the

- mid-holocene and the last glacial maximum, *Quaternary Science Reviews* 156 (2017) 107 – 120. doi:<https://doi.org/10.1016/j.quascirev.2016.11.028>.
- 600 [46] A.-M. Lézine, C. Hély, C. Grenier, P. Braconnot, G. Krinner, Sahara and Sahel vulnerability to climate changes, lessons from Holocene hydrological data, *Quaternary Science Reviews* 30 (21) (2011) 3001–3012. doi:<https://doi.org/10.1016/j.quascirev.2011.07.006>.
- [47] T. Bischoff, T. Schneider, A. N. Meckler, A conceptual model for the response of tropical rainfall to orbital variations, *Journal of Climate* 30 (20) 605 (2017) 8375–8391. arXiv:<https://doi.org/10.1175/JCLI-D-16-0691.1>, doi:10.1175/JCLI-D-16-0691.1. URL <https://doi.org/10.1175/JCLI-D-16-0691.1>
- [48] O. Adam, T. Schneider, F. Brient, Regional and seasonal variations of the double-ITCZ bias in CMIP5 models, *Climate Dynamics* 51 (2018) 101–117. 610 doi:10.1007/s00382-017-3909-1.
- [49] A. Donohoe, J. Marshall, D. Ferreira, D. McGee, The relationship between ITCZ location and cross-equatorial atmospheric heat transport: From the seasonal cycle to the last glacial maximum, *J. Climate* 26 (2013) 3597–3618.
- 615 [50] A. Donohoe, D. S. Battisti, The seasonal cycle of atmospheric heating and temperature, *J. Climate* 26 (2013) 4962–4980.
- [51] T. M. Merlis, T. Schneider, S. Bordoni, I. Eisenman, Hadley circulation response to orbital precession. Part I: Aquaplanets, *J. Climate* 26 (2013) 740–753.
- 620 [52] D. M. W. Frierson, Y.-T. Hwang, N. S. Fuckar, R. Seager, S. M. Kang, A. Donohoe, E. A. Maroon, X. Liu, D. S. Battisti, Contribution of ocean overturning circulation to tropical rainfall peak in the northern hemisphere, *Nature Geosci.* 6 (2013) 940–944. doi:10.1038/ngeo1987.

- [53] Y.-T. Hwang, D. M. W. Frierson, Link between the double-Intertropical
625 Convergence Zone problem and cloud biases over the Southern Ocean, *Proc.
Natl. Acad. Sci.* 110 (2013) 4935–4940. doi:10.1073/pnas.1213302110.
- [54] A. Donohoe, J. Marshall, D. Ferreira, K. Armour, D. McGee, The in-
terannual variability of tropical precipitation and interhemispheric energy
transport, *J. Climate* 27 (2014) 3377–3392.
- 630 [55] M. J. Rodwell, B. J. Hoskins, Monsoons and the dynamics of deserts, *Quart.
J. Roy. Meteor. Soc.* 122 (1996) 1385–1404.
- [56] H. Su, D. Neelin, Dynamical mechanisms for African monsoon changes
during the mid-Holocene, *J. Geophys. Res.* 110 (2005) D19105.
- [57] D. P. Rowell, The impact of mediterranean ssts on the Sahelian rain-
635 fall season, *Journal of Climate* 16 (5) (2003) 849–862. doi:10.1175/
1520-0442(2003)016<0849:TIOMS0>2.0.CO;2.
- [58] Y. Zhao, P. Braconnot, O. Marti, S. Harrison, C. Hewitt, A. Kitoh,
Z. Liu, U. Mikolajewicz, B. Otto-Bliesner, S. Weber, A multi-model anal-
ysis of the role of the ocean on the African and Indian monsoon dur-
640 ing the mid-Holocene, *Climate Dynamics* 25 (7) (2005) 777–800. doi:
10.1007/s00382-005-0075-7.
- [59] C. Lavaysse, C. Flamant, S. Janicot, D. J. Parker, J.-P. Lafore, B. Sul-
tan, J. Pelon, Seasonal evolution of the west African heat low: a cli-
matological perspective, *Climate Dynamics* 33 (2) (2009) 313–330. doi:
645 10.1007/s00382-009-0553-4.
- [60] S. E. Nicholson, The West African Sahel: A review of recent studies on the
rainfall regime and its interannual variability, *ISRN Meteorology* (453521)
(2013) 32pp. doi:10.1155/2013/453521.
- [61] R. Shekhar, W. R. Boos, Weakening and shifting of the Saharan shallow
650 meridional circulation during wet years of the West African monsoon, *J.
Climate* 30 (2017) 7399–7422. doi:10.1175/JCLI-D-16-0696.1.

- [62] O. Adam, T. Schneider, F. Brient, T. Bischoff, Relation of the double-ITCZ bias to the atmospheric energy budget in climate models, *Geophys. Res. Lett.* 43 (2016) 7670–7677.
- 655 [63] J. A. Collins, E. Schefuß, D. Heslop, S. Mulitza, M. Prange, M. Zabel, R. Tjallingii, T. M. Dokken, E. Huang, A. Mackensen, M. Schulz, J. Tian, M. Zarriß, G. Wefer, Interhemispheric symmetry of the tropical African rainbelt over the past 23,000 years, *Nature Geoscience* 4 (2011) 42–45. doi:10.1038/ngeo1039.
- 660 URL <http://dx.doi.org/10.1038/ngeo1039>
- [64] H. Yan, W. Wei, W. Soon, A. Zhisteng, W. Zhou, Z. Liu, Y. Wang, R. Carterm, Dynamics of the intertropical convergence zone over the western Pacific during the Little Ice Age, *Nature Geoscience* 8 (2015) 315–320.
- [65] A. C. Clement, R. Burgman, J. R. Norris, Observational and model evidence for positive low-level cloud feedback, *Science* 325 (2009) 460–464.
- 665 [66] O. Boucher, D. Randall, P. Artaxo, C. Bretherton, G. Feingold, P. Forster, V.-M. Kerminen, et al., Clouds and aerosols, in: *Climate Change 2013: The Physical Science Basis*, Intergovernmental Panel on Climate Change, 2013, Ch. 7.
- 670 [67] G. Lohmann, M. Pfeiffer, T. Laepple, G. Leduc, J. Kim, A model-data comparison of the holocene global sea surface temperature evolution, *Climate of the Past* 9 (4) (2013) 1807–1839. doi:10.5194/cp-9-1807-2013.
- [68] B. Molfino, A. McIntyre, Precessional forcing of nutricline dynamics in the equatorial atlantic, *Science* 249 (4970) (1990) 766–769. doi:10.1126/science.249.4970.766.
- 675 [69] S. Weldeab, D. W. Lea, R. R. Schneider, N. Andersen, 155,000 years of west african monsoon and ocean thermal evolution, *Science* 316 (5829) (2007) 1303–1307. doi:10.1126/science.1140461.

- [70] J. E. Kutzbach, Monsoon climate of the early holocene: Climate experiment
680 with the earth's orbital parameters for 9000 years ago, *Science* 214 (4516)
(1981) 59–61. doi:10.1126/science.214.4516.59.
- [71] A. C. Clement, A. Hall, A. J. Broccoli, The importance of precessional
signals in the tropical climate, *Climate Dyn.* 22 (2004) 327–341.
- [72] D. S. Battisti, Q. Ding, G. H. Roe, Coherent pan-asian climatic and iso-
685 topic response to orbital forcing of tropical insolation, *Journal of Geo-
physical Research: Atmospheres* 119 (21) (2014) 11,997–12,020. doi:
10.1002/2014JD021960.
- [73] W. R. Boos, R. L. Korty, Regional energy budget control of the intertropical
690 convergence zone and application to mid-Holocene rainfall, *Nature Geo-
science* 9 (2016) 892–897. doi:10.1038/ngeo2833.